2010 IEEE International Conference on Robotics and Automation
Anchorage Convention District
May 3-8, 2010, Anchorage, Alaska, USA

A Multiple SMA Hybrid Actuator to Generate Expressions on the Face

Dushyantha Jayatilake, *Student member, IEEE* and Kenji Suzuki, *Member, IEEE*

Abstract— **This paper presents part of an on-going project to design a wearable supportive device to enhance facial expressiveness, in particular for the facial paralyzed patients. Earlier we introduced the SMA actuator based Robot Mask that can be used to enhance the expressiveness of the face. The basic concept of that design was pulling of the skin through wires attached to the face and we explained the human anatomy based criteria of selecting these pulling points and directions. The major reason to use SMA instead of traditional actuators such as motors was their silent acting nature. However, their dynamic properties been governed by thermal energy and their mechanical properties been affected by the hysteresis due to their metallurgy, SMA based actuators tend not to perform too well under cooling. This paper introduces a novel controlling scenario that use the actuation of only a limited number of SMA wires out of the total connected in series on either sides of a slider to control the direction and amount of movement of the slider. The advantage of this method is by keeping some SMA wires at low temperatures it was possible to achieve a high speed of actuation even when the direction of motion was changed. This paper also investigates on the amount of actuation rates that are required to generate natural looking smiles and later attempts to recreate them using the proposed actuation unit.**

Index Terms— **SMA, Facial Expressiveness, Segmented Hybrid Control**

I. INTRODUCTION

Non-verbal communication based information exchange is significantly important in social communication. Mostly simple, these expressions are easily understood by almost everybody and more extensively by the members of the local social community. In general they are said to be globel, although there are reports of culturally dependent expressions and socially modified versions of universal expressions [1]. Among the many varieties of expressions of non-verbal communication such as gestures, physical contact, body language, and eye contact etc., facial expressions are of paramount importance. During face to face communication, the partners are most likely to look towards each other, making facial expression more easily recognizable compared to other expressions [2].

Facial expressions, which are governed by the decisions initiated at the brain and sent through the facial nerve as electrical signals are produced by the actions of the facial muscles [3]. However due to various complications, these muscle activities can sometimes degrade or even disappear resulting in the condition called the facial paralysis. The effects of facial paralysis could be temporary or permanent as well as the affected area could be concentrated to a small area, one side of the face or both sides of the face. Consequences of facial paralysis could be devastating in many a ways. Apart from being facially less responsive, it can dramatically change the shape of the face [4]. In particular under single side or hemifacial paralysis, the drooping of the ipsilateral face due to absence of muscle tension and the consequent deviation of the nose to the contralateral side of the face will result in loosing the baseline muscle tone and results in destroying the symmetry of the face [5].

Although medical support is available for such patients to speed up the healing process, as temporary paralysis sometimes can last up to 2 to 3 years, it is necessary to have some other means to provide immediate relief. Robot Mask is the device that we have been developing to generate facial expressions artificially. It basically consists of a head supporter, a pulling wire arrangement, a bioelectrical signal extraction unit, motor units with control a unit and a power supply unit. Each motor actuation unit have there own built in dedicated control unit and a common controller is used to integrate them in to the main system. As it can be seen from Fig. 1, the basic idea of the device is the pulling of facial skin towards carefully selected directions by using wires attached to the facial skin at carefully selected points. We have described the anatomy based selection of these points and directions in our earlier papers [6], [7]. In the initial version of the Robot Mask which concentrates on the hemifacial paralysis, the bioelectrical signal extraction unit is positioned near the Parotid Gland of the contralateral face and the processed bioelectrical signal is used to generate similar expressions on the ipsilateral face.

As it was described previously, the facial expressions are a part of non verbal communication and therefore one of the key characteristic of them are the silence. Hence it is fairly difficult to use traditional motor based actuators to generate facial expressions since some mechanical noises are always associated with them. Shape Memory Alloys (SMA) on the other hand are not only silent, but they also provide much more such as high weight to power ratio and compactness etc. However one major disadvantage of SMA, which is due to its metallurgy is its weakness during cooling. This is mainly caused by the significant hysteresis in the strain-temperature, stress-strain and resistance-temperature relations of the SMA [8], [9].

In this study, helically wound 0.15 [mm] diameter Ni-Ti-

This study was supported in part by the Global COE Program on "Cybernics: fusion of human, machine, and information systems" at the University of Tsukuba and also Grant-in-Aid, Yoshikawa-Ozawa Memorial Foundation for Electronics.

D. Jayatilake (dush@ieee.org) and K. Suzuki (kenji@ieee.org) are with the Artificial Intelligence Laboratory of the Graduate School of Systems and Information Engineering of University of Tsukuba, Japan.

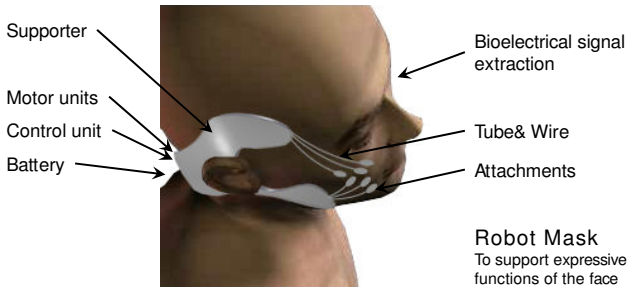

Fig. 1. The overview of the Non Invasive Robot Mask with six degrees of freedom of actuation

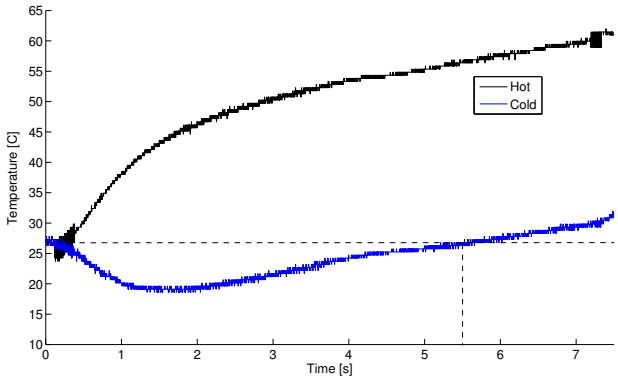

Fig. 2. Peltier device surface temperature variation: 30×30 [mm] peltier operating at an input power of 5 [W] with a thermally loaded SMA wire lying on top of it.

Cu based SMA were used in the actuators. This particular 0.62 [mm] diameter SMA helices have a specific heat value of 6.1 [cal/mol°C] at martensite low temperature phase and 8 [cal/mol°C] at austenite high temperature phase and under normal working conditions the actuators were found to be operating around 68°C (the temperature data were recorded using a Chromel-Alumel K type thermocouple and a AND AD-5602 thermometer). Although compared to SMA fibers, SMA helices are not superior with respect to load carrying capacity, they are capable of producing large kinetic distortions of 100% or more.

This paper presents a novel linear actuator design for a facial expression generator, which is based on SMA segments connected in series that can provide quick motion in both directions. It explains how the strategy could help to reduce the effects of slow cooling in SMA based actuators. A performance comparison is done for a step reference input against a single SMA actuator. The paper also analyses the facial skin change during smile and attempts to recreate that smile profile with the new actuators.

II. ACTUATOR

Actuators for the Robot Mask demands unique set of design and operating constraints. They should be small, light and fast in response. They don't need to carry large loads (around 140 [gf] would be adequate [6]), however they need to have good position controllability. Maximum actuation amounts of the range of 18 [mm] would be adequate, although typically it is much less (around 10 [mm]) [7]. However it is necessary to have at least point to point controllability of the order of 1 [mm].

The actuators of the Robot Mask that were introduced in our previous publications are capable of generating a facial expression within 2.5 seconds. However their returning to neutral state is relatively slow and at time it can take as many as $8 \sim 10$ seconds [10]. This is due to the absence of an artificial cooling method inside the actuation unit. In order to overcome this cooling issue associated with SMA, Asada et.al. (2003) have proposed an actuator which is immersed in a flow of water [11]. However, the relatively large size of that cooling unit makes it undesirable for the current application. Another possibility would be the use of Peltier devices to cool the SMA wire [12], [13]. However as shown in Fig. 2, we noticed that in a Peltier device when the heat is not removed from the hot surface, due to the heat transfer from hot surface to cold surface, the cold surface starts to get warmer (after 1.5 [s] in this experiment) and could even become warmer than the atmospheric temperature in turn minimizing the effect of artificial cooling. The data was taken by mounting two S-8100B CMOS (-8.1 [mV/K]) surface temperature sensors on either sides of the Peltier device. In order to use them effectively, some heat removal mechanism such as a heat sink and/or a fan is required. However, such usage essentially contradicts with the fundamental concept of silent actuation, which is the main reason to use SMA instead of motors.

Consequently in this study, we propose a segmentally controlled bidirectional actuation unit to generate facial expressions for real time communication. Main feature of this unit is the controlling algorithm which quickens the reversal of direction of motion by keeping one actuator at a lower temperature, there by reducing its cooling time. The other major difference is the use of encoders to obtain the actual displacement produced by the contraction of SMA which contrasts to the approach of using SMA mechanical properties to mathematically deduce the amount of contraction which is used by most other researchers [8], [14].

A. Construction of the Actuator

Fig. 3 shows the design of the Silent Actuation Unit (SIAC). It consists of five slider elements sliding along the groves of the external guiding unit. The bottom side of the main slider is fitted with the linear encoder strip of the reflective type 150 [line/inch] optical encoder, where as the encoder is mounted on the guiding unit, right beneath the slider. The other four slider elements sliding on the guiding unit are denoted by there representatives voltages, V_1, V_2, V_3, and V_4. The helically wound SMA wire, which is held at the ends of the SIAC guiding unit is tapped to all five sliders. The main slider and the four minor sliders make three bays

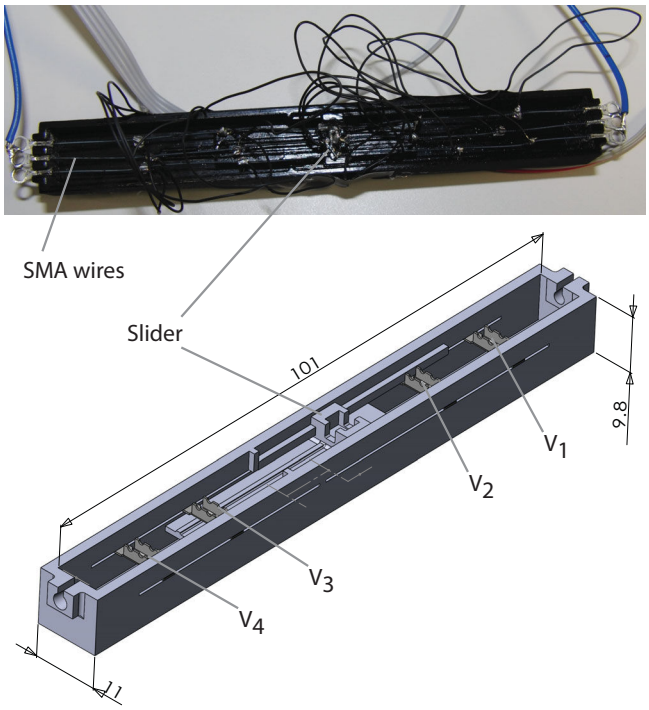

Fig. 3. An image and the 3D CAD drawing of the experimental model of the actuator.

each for either direction and the load is connected to the main slider. The minor sliders are mainly there to support the length of the SMA wire and facilitate its electrical supply. The Joule heating supplied through electrical currents is used to heat up the SMA wire. The two ends of the SMA wire and the main slider are connected to electrical ground and the potentials on four minor sliders are controlled by the position controlling algorithm. Because of this special wiring structure, when the actuator is working at a certain direction, it is alway possible to keep any of the three SMA segments either at a low or even zero potential there by making it more flexible compare to other two and when the slider direction is reversed, that particular segment will act like a low stiff spring making it easier to reverse the direction of motion.

B. Controlling algorithm

Although bidirectional actuation based SMA actuators have already been tested [15], a definite solution to the problem associated with the relatively slow cooling rate of SMA has not been found yet. For instance, when heated from a 5 [V] electrical supply, the 0.15 [mm] diameter and 40 [mm] long spring wound SMA wire used in the current study, on average exhibited a cooling rate of 3.3 [°C/s] opposed to relatively high heating rate of 6.5 [°C/s]. To overcome this problem, a hybrid architecture of segmented SMA in bidirectional actuation that can conveniently generate both the motions; expansion and compression was tested in this study. The digital control system was implemented on a Microchip™ dsPIC33F128MC802 microprocessor and a sampling interval of 20 [ms] was used in the digital control

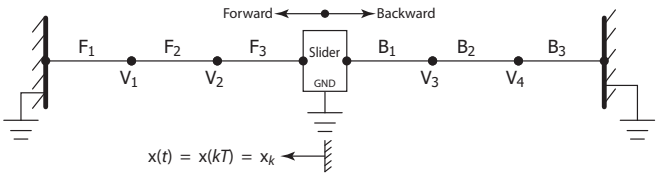

Fig. 4. Multi SMA actuation model

TABLE I
SMA DRIVING CONFIGURATIONS

	Forward		Backward	
	V_1	V_2	V_3	V_4
$Case\ A$	$0.85\,V_t$	V_t	0	0
$Case\ B$	V_t	0	0	0
$Case\ C$	0	V_t	0	0
$Case\ D$	0	0	V_t	0
$Case\ E$	0	0	0	V_t
$Case\ F$	0	0	V_t	$0.85\,V_t$

algorithm with the feedback being taken by a 150 [lines/inch] Avago™ AEDR-8300 optical encoder. A 2 [kHz] pulse width modulation (PWM) signal was used to generate the driving signal and P-channel logic level MOSFET were used to drive the SMA load. By taking in to account the high thermal inertia of SMA, the PWM signal was directly used to drive the load.

Actuation Conditions

Based on the electrical connection and power up circuit of the SIAC unit, six different configurations, namely A, B, C, D, E, and F are used to drive the actuator. The cases are selected such that in any given instance, actuation is done only at one direction, either forward or backward. Table I outlines the complete set of driving configurations used in the controlling algorithm. V_t indicates the variable voltage at time t.

$Case\,A$ indicates a situation where ends of the middle actuator for forward direction F_2 has only a very small potential difference, resulting in the actuation of almost only F_1 and F_3. The Joule heating provided from the small potential difference helps to keep the middle SMA stiff while ensuring a quicker cooling due to low temperature. In $Case\,B$, setting both the slider and V_2 at ground potential results in actuating only F_1 and F_2. $Case\,C$ corresponds to the actuation of only F_2 and F_3. The backward direction cases work in a similar manner, always enabling only two out of the three actuators that can generate the desired motion.

C. Controlling Scenario

When sampling period is T, denoting the reference input value x_{ref} at the k^{th} sampling interval as x_{ref_k}, the controlling approach could be mainly divided in to two instances, $x_t \leq x_{ref_k}$ and $x_t > x_{ref_k}$, where $x_t = x(kT)$ represents the location of the slider at time t and each of those

two instances could be further subdivided in to two more instances each as, $x_{ref_k} \neq x_{ref_{k-1}}$ and $x_{ref_k} = x_{ref_{k-1}}$.

1) *if* $x_t > x_{ref_k}$

   Enable pulse width modulation (PWM) on channels 3 and 4 (V_3 and V_4) and disable PWM on channels 1 and 2 (V_1 and V_2) enabling the backward motion while putting the forward motion actuators at rest.

   Calculate the current position as,

   $\hat{x}_t = 2x_{ref_k} - x_t$

   if $\hat{x}_t < 0 \rightarrow \hat{x}_t = 0$

   else

   Enable PWM on channels 1 and 2 and disable PWM on channels 3 and 4 (this enables the forward motion while putting the reverse motion actuators at rest)

   Set the current position $\hat{x}_t = x_t$

2) Using $\hat{x}_t$ as the current position, calculate the controller output U_k for the PID controller
3) Select "Actuation Case"
4) Load U_k to PWM duty ratio controller

Of the six actuators, represented by F_i and B_i $(i = 1, 2, 3)$, for $x_{ref_k} > 0$ only two actuators are active at any given instance. At the beginning, $i = 1$ and 2 are selected as default working actuators by the "Actuation Case" process, whereas upon a change of slider moving direction, the subsequent working actuators are selected with respect to two conditions.

During normal continuous operation, a timer is initiated at the start of a change in direction of motion of the slider and a cooling flag C^f which is set at a timer overflow is used to indicate sufficient cooling of actuators bound to the opposite direction that were in action prior to the previous change of direction of motion. At the next change of direction of motion, depending on desired direction of motion, after determining F_i or B_i, the cooling flag is checked for the completion of cooling. If the flag is set, since the duration of the current action has allowed enough cooling time for the previous set of actuators that were in use, the same set of actuators are used for the next action. If the cooling is not sufficient, depending on the desired direction of motion, the next set of actuators are selected cyclically between the cases $A \rightarrow B \rightarrow C$ or $D \rightarrow E \rightarrow F$. If F_is are in action, B_is are at rest and vice-versa. When the slider is moving in one direction the SMA wires intended for the opposite direction are maintained at unused state. However, during operation for which $x_{ref_k} = x_{ref_{k-1}}$, in order to maintain smoothness, the PID control output for them are updated regularly. This helped to reduce the overshoot and fluctuations.

D. Fast Actuation and Prevention of Overheating

At the beginning, the PWM modules are initialized with a 100% duty ratio, making it possible to pump the largest possible current in to the SMA wire there by achieving the fastest possible initial actuation. However, during the operation, the duty ratios are adjusted by the PID control unit to achieve desired position control. Nevertheless, when

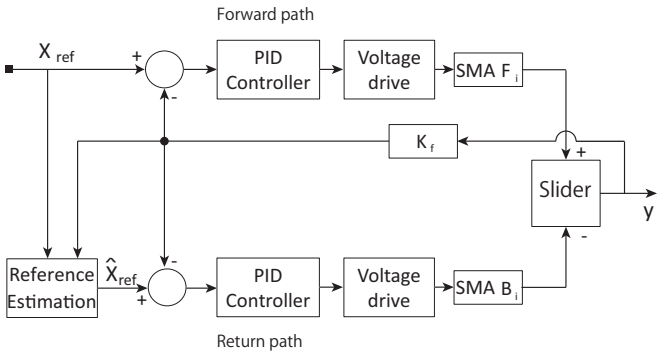

Fig. 5. Block diagram of forward and return twin path control system.

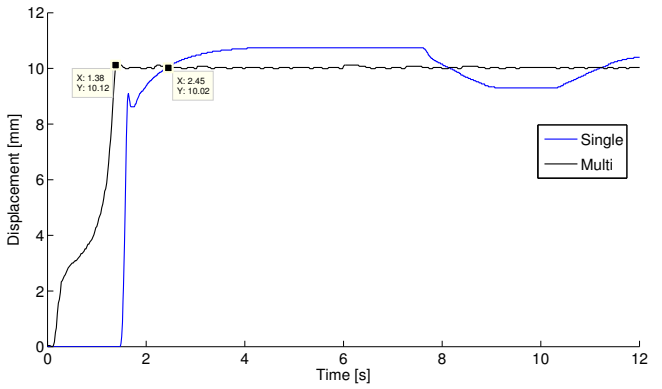

Fig. 6. Actuator response to a 10 [mm] step input

the actuators are used at the same direction for a rather longer duration, due to the payload followed by the cooling down of low powered SMA segment and the consequent loosing of stiffness, that segment is likely to elongate, negating the effect of other two SMA segments in action. This loose of contraction in turn will result in the PID controller increasing its duty ratio on those two actuators and persevering such high duty ratios are likely to cause the SMA segments to overheat. The same cooling flag C^f is used to rectify such issues. In this instance, upon the setting of C^f if the direction change flag D^f has still not been set, that forces a change in actuation case while maintaining the actuation direction. This mechanism will helps to maintain the stiffness of all the loading direction actuators above a critical level k_L^{Cr}, while ensuring that no SMA segment will be used for more than twice the minimum required cooling period.

Fig. 5 shows the block diagram of the position control system. It consists of two parallel loops that takes care of forward and backward motions separately. In the forward motion loop, the position error is sent to the PID controller. 0.85, 0.5, and 0.75 are used as the gain parameters K_p, K_d, and K_i of the forward control path, whereas taking in to account the support of skin weight during return motion, relatively slower parameters of 0.6, 0.45 and 0.6 are used in the return control loop. Since overshoot is not a serious

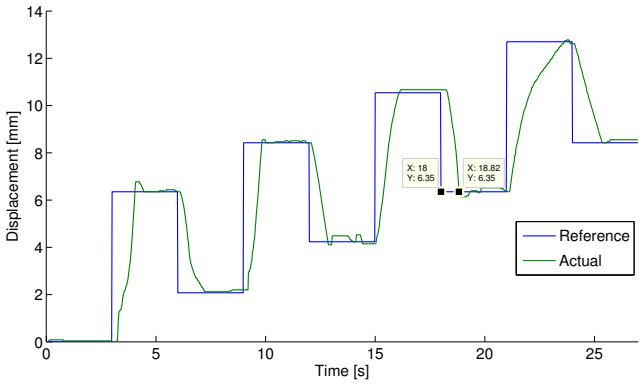

Fig. 7. Actuator response to a step type varying input

problem as logically controlled actuation direction changes at the reference point, through manual on-line tuning, the initial values of PID gain parameters were selected to have a fast rise time. Hardware based but software controlled encoder feedback gain was selected as 600 pulses per inch (ppi).

Fig. 6 shows the actuator characteristics for a 10 [mm] step type reference input. The two graphs are the new bidirectional segmentally controlled actuator denoted by "Multi" and the unidirectional single SMA actuator denoted by "Single". As it can be seen, the new actuator performs much faster than the Single design reducing the rise time by almost 44% (1.38 [s] compared to 2.45 [s]) with almost negligible amount of overshoot (1.6% compared to 7.4%). This fast start is characterized by the high initial duty ratio loaded to the PWM module.

Fig. 7 shows the new actuator performances against a step wise varying input. The input is a $1/4$ [inch] up followed by a $1/6$ [inch] down with 3 [s] intervals between them. As it can be seen from the figure, with even the return stroke taking less than 1 [s] in general, the actuator performs exceptionally well both in forward and return strokes with a minimum of overshoot and fluctuations.

III. Performance Evaluation on the Face

In order to evaluate the suitability of the new proposed algorithm as a facial expression generator, we initially measured the displacement characteristics of the facial skin. Since skin displacement characteristics varies from expression to expression as well as person to person, it is difficult to generate a universal reference expression. Hence as a pilot study, only the smile characteristics along the *Zygomaticus major* muscle direction of an adult male subject was evaluated in this study. The left most figure of Fig. 8 shows the position of the *Zygomaticus major* muscle. This muscle is mainly used to raise the mouth corner during smiling. The displacement profile for a random smile action, as the one shown in Fig. 9 was obtained by attaching a linear encoder to the face. We previously showed that for small displacements, the linear ditance between the starting and

Fig. 8. Analyzing of skin movement along *Zygomaticus major* direction

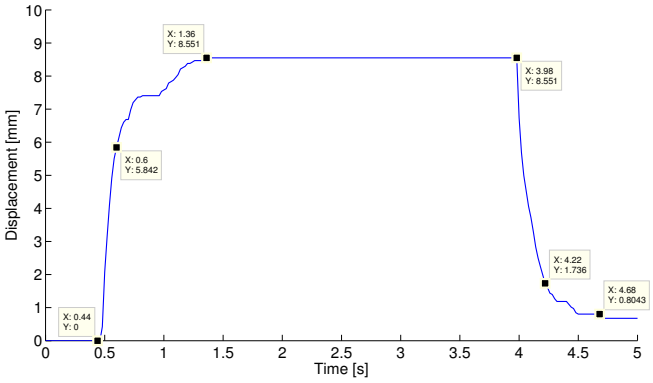

Fig. 9. Smile profile along *Zygomaticus major* direction

the final point measured from such a sensor is similar to the 3D displacement [7], [10].

Fig. 9 shows the displacement variation against time for that action. The expression can be considered as a regular smile and as it can be seen from the figure the smile action normally finishes in about 0.9 [s]. After holding the smile for about 2.6 [s] it gradually descends back to the neutral state with major part of the descending process finishing within 0.5 [s].

Fig. 10 shows the reproduction of natural smile by the actuators of the Robot Mask. As it can be seen from the figure although the shape of the profiles resembles each other, as expected the artificially recreated smile always lags behind the natural smile. However, the amounts they are lagging behind are not too large and therefore the artificial expression could be considered as a slow response to the natural smile. Furthermore, when considered the delay between nerve signals and the muscle actions and then the bioelectrical signal based actuation mechanism proposed in the Robot Mask, we can reasonably assume that the gap between natural and artificial responses could be even smaller.

IV. Conclusions and Future Works

A. Conclusions

This paper introduced an SMA based actuator control method which use the advantages of both bidirectional

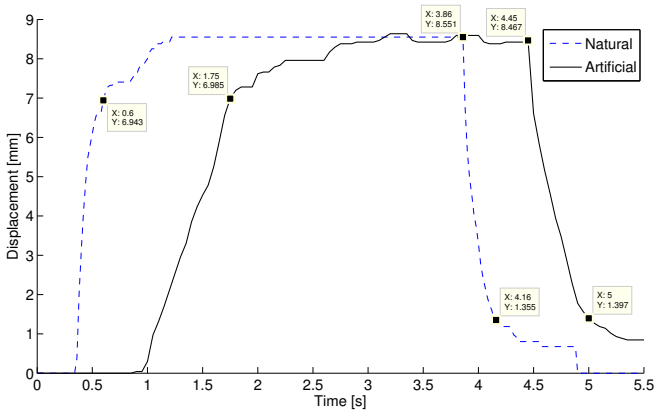

Fig. 10. Reproduction of smile profile by the new actuator

actuation and segmented control for the previously presented Robot Mask system. Initial high current injecting algorithm helped to reduce the starting delay and resulted in a 44% reduction of rise time for a 10 unit step input. By keeping some SMA segments at lower temperatures during actuations, we were able to achieve quicker reversing times which is important for the "Robot assisted smile recovery". Updating of controlling parameters even of the rested SMA segments worked as an annealing process helping to improve the smoothness of the actuation. The actuator which use real position feedback showed good position controllability as well as much improved actuation characteristics during both expansion and compression. The step response too was much faster with negligible amounts of overshoot and fluctuations.

A smile based performance evaluation showed although the response is slightly slow and delayed, still good enough to be considered as a slow smile.

In this study the critical temperature of the low heated SMA segment k_L^{Cr} was selected arbitrarily by the trial and error changing of the cooling time. However, establishing it through a more logical basis such as by a mathematical model could help to optimize the performance.

B. Future Works

In order to optimize the controller performances we plan to model the heat transfer into the SMA segments as well as the stiffness variation against environmental variables. This could yield to better selection of C^f timer overflow values and much better idling state temperature (PWM duty ratio) values. We also plan to work on the reduction of the actuator size and power consumption as well as prolonging its life as they are very important to the successful implementation of the Robot Mask system.

V. ACKNOWLEDGMENTS

This study was supported in part by the Global COE Program on "Cybernics: fusion of human, machine, and information systems" at the University of Tsukuba and also Grant-in-Aid, Yoshikawa-Ozawa Memorial Foundation for Electronics.

REFERENCES

[1] P Ekman. Facial expressions of emotion: an old controversy and new findings. *Philosophical Transactions of the Royal Society of London*, 335:pp. 63–69, 1992.

[2] U. Dimberg and B. Karlsson. Facial reactions to emotionally relevant stimuli. *Skandinavian Journal of Psychology*, 38:297–303, 1997.

[3] A.F. Dalley A.M.R. Agur. *"Grant's Atlas of Anatomy"*. Lippincott Williams and Wilkins, eleventh edition edition, 2005.

[4] Barry M. Schaitkin Mark May. *Facial Paralysis: Rehabilitation Techniques*. Thieme, 2003.

[5] Myles L. Pensak. *Controversies in Otolaryngology*. Thieme, first edition edition, 2001.

[6] D. Jayatilake and K. Suzuki. A soft actuator based expressive mask for facial paralyzed patients. *Intelligent Robots and Systems, 2008. IROS 2008. IEEE/RSJ International Conference on*, pages 4048–4053, Sept. 2008.

[7] Dushyantha Jayatilake, Anna Gruebler, and Kenji Suzuki. An analysis of facial morphology for the robot assisted smile recovery. *Information and Automation for Sustainability, 2008. ICIAFS 2008. 4th International Conference on*, pages 395–400, Dec. 2008.

[8] Nagarajan T. Zoppi M. Sreekumar M., Singaperumal M. and Molfino R. Recent advances in nonlinear control technologies for shape memory alloy actuators. *Zhejiang University Press, Co-published with Springer-Verlag GmbH*, Volume 8:818–829, April 2007.

[9] C.L. Gu K. Yang. Modelling, simulation and experiments of novel planar bending embedded sma actuators. *Special Section of Revised Papers from the 8th International IFAC Symposium on Robot Control, 8th International IFAC Symposium on Robot Control, ScienceDirect*, Mechatronics Volume 18(Issue 7):323–329, September 2008.

[10] Dushyantha Jayatilake, Keisuke Takahashi, and Kenji Suzuki. An assistive mask with biorobotic control to enhance facial expressiveness. In *Intelligent Robots and Systems, 2009. IROS 2009. IEEE/RSJ International Conference on*, pages 3568–3573, Oct. 2009.

[11] H.H. Mascaro, S.A. Asada. Wet shape memory alloy actuators for active vasculated robotic flesh. *Proc. of ICRA '03, IEEE International Conference on Robotics and Automation*, Volume 1:pp. 282–287, Sep. 2003.

[12] Kyu-Jin Cho and H.H. Asada. Segmentation architecture of multi-axis sma array actuators inspired by biological muscles. In *Intelligent Robots and Systems, 2004. (IROS 2004). Proceedings. 2004 IEEE/RSJ International Conference on*, volume 1, pages 254–259 vol.1, Sept.-2 Oct. 2004.

[13] Kyu-Jin Cho and H. Asada. Multi-axis sma actuator array for driving anthropomorphic robot hand. In *Robotics and Automation, 2005. ICRA 2005. Proceedings of the 2005 IEEE International Conference on*, pages 1356–1361, April 2005.

[14] B. Selden H. H. Asada, K. J. Cho. Shape memory alloy actuator system using segmented binary control. Technical Report Patent No.: US 7188743 B1, United States Patents, Mar. 13 2007.

[15] F. Nakazawa D. Homma, S. Uemura. Functional anisotropic shape memory alloy fiber and differential servo actuator. *SMST-2007: Proceedings of the International Conference on Shape Memory and Superelastic Technologies*, pages 463–471, Nov. 2008.